Supporting Information

A Facile Room-Temperature Fabrication of Silver-Platinum Nanocoral Catalyst Towards Hydrogen Evolution And Methanol Electro-Oxidation

Hau Quoc Pham,[1,2] and Tai Thien Huynh[3,]*

[1]Future Materials & Devices Lab., Institute of Fundamental and Applied Sciences, Duy Tan University, Ho Chi Minh City, 700000, Viet Nam

[2]The Faculty of Environmental and Chemical Engineering, Duy Tan University, Da Nang, 550000, Viet Nam

[3]Ho Chi Minh City University of Natural Resources and Environment (HCMUNRE), Ho Chi Minh City, 700000, Viet Nam

*Corresponding author. E-mail: httai@hcmunre.edu.vn

EXPERIMENTAL DETAILS

Chemical reagents

All reagents were commercially purchased and used without further purification. Hexachloroplatinic acid ($H_2PtCl_6.xH_2O$; ~38% Pt), silver nitrate ($AgNO_3$; ≥99.0%), and Nafion 117 solution (~5%) were purchased from Sigma-Aldrich, USA. Formic acid (HCOOH; 98-100%), ethanol absolute (C_2H_5OH; 99.5%), sulfuric acid (H_2SO_4, 95-97%); and methanol (CH_3OH) were obtained from Merck, Belgium.

Material Characterizations

X-ray diffraction (XRD) analysis was performed on a D2 PHASER (Bruker, Germany) using Cu K_α radiation source (λ = 1.5418 Å) in the 2θ range from 20° to 80° at a step size of 0.02° to collect the structure information of as-obtained catalysts. X-ray photoelectron spectroscopy (XPS) was analyzed on PHI 5000 VersaProbe (Ulvac-PHI) equipped with monochromator Al K_α ($h\upsilon$ = 1486.6 eV) X-ray source at a 10 mV current and 15 kV anode voltage. The morphology and size of the AgPt nanocatalyst were recorded through transmission electron microscopy (TEM) and HR-TEM images, which were carried out on a JOEF-JEM 2100F device at 200 kV. Before TEM measurement, the sample was dispersed in ethanol to generate a homogeneous suspension, which was cast on carbon film-coated copper microgrids.

The coherent length ($D_{(hkl)}$) was estimated by Debye-Scherrer's formula (Eq.(1))[1-3]:

$$D_{(hkl)} = \frac{k\lambda}{\beta\cos\theta} \qquad \text{(Eq. (1))}$$

where: $D_{(hkl)}$ is average crystallite size (nm); k is Scherrer constant (0.94), λ is the wavelength of the incident X-ray (λ = 15406 Å); β is the line broadening at half the maximum intensity (FWHM), and θ is the Bragg angle.

The lattice space ($d_{(hkl)}$) was calculated by Bragg's law (Eq. (2))[2, 3]

$$d_{(hkl)} = \frac{\lambda}{2\sin\theta} \quad \text{(Eq. (2))}$$

where: $d_{(hkl)}$ is lattice space (Å); λ is the wavelength of the incident X-ray (λ = 15406 Å); θ is the Bragg angle.

Electrochemical Properties

Electrochemical tests were performed on a CHI 660 C Electrochemical Workstation (CH Instruments Inc., USA) connected with a three-electrode electrochemical cell consisting of a glassy carbon electrode (GCE), platinum wire, and Hg/HgO electrode, which were used as a working electrode, a count and reference electrodes, respectively. In terms of the catalyst ink fabrication, 1.7 mg of catalyst was distributed in a mixture of 20 μL of Nafion and 180 μL of ethanol absolute, followed by the ultrasonication of 30 min to generate a homogeneous ink. To coast the obtained catalyst ink, the GCE surface was polished by 0.5 μm Al_2O_3 and washed by absolute ethanol and purged water, and then 2.5 μL of catalyst ink was drop-cast onto the GCE surface and dried naturally, followed by scanning in N_2-saturated 0.5 M H_2SO_4 at 50 mV s^{-1} for 100 cycles to get an active working electrode. The electrochemical surface area (ECSA) of investigated catalyst was estimated from hydrogen adsorption/desorption region in cyclic voltammetry (CV) in N_2-saturated 0.5 M H_2SO_4 aqueous electrolyte at 25 mV s^{-1} scan rate. The electrocatalytic performance towards hydrogen evolution reaction (HER) of catalysts was measured by linear sweep voltammetry (LSV) in N_2-saturated 0.5 M H_2SO_4 at a 1 mV s^{-1} scan rate. Electrochemical impedance spectroscopy (EIS) of electrocatalysts was collected at an amplitude of 5 mV in the frequency range from 0.1 to 10^5 Hz. In addition, the electrocatalytic activity towards methanol electro-oxidation reaction (MOR) of as-prepared catalyst was examed in N_2-saturated 0.5 M H_2SO_4 + 1.0 M CH_3OH aqueous solution by CV and LSV tests. CO-stripping test was performed in 0.5 M H_2SO_4 electrolyte, which was purged with nitrogen gas for 15 min and then CO gas bubbled for 45 min at 0.05 V_{RHE}. In terms of the electrocatalytic

stability, chronoamperometry (CA) at fixed 0.7 V_{RHE} and accelerated durability test (ADT) with the 2000-cycling test were also used. For comparison, the commercial Pt NPs/C (E-TEK) was used as a benchmark catalyst. All potential in this work was converted to a reversible hydrogen electrode (RHE) through the Nernst equation.

Electrochemical surface area (ECSA) calculation

The electrochemically surface area (ECSA) of Pt-based electrocatalyst was calculated from hydrogen adsorption/desorption regions in cyclic voltammetry (CV) curve in N_2-saturated 0.5 M H_2SO_4 electrolyte according to Eq. (3) [4-6]:

$$ECSA=\frac{Q_H}{0.21*[Metal]} \quad \text{(Eq. (3))}$$

where Q_H (mC cm^{-2}) represents the coulombic charge for hydrogen adsorption; 0.21 (mC cm^{-2}) is the charge required to oxidize an H_2 monolayer, and [Metal] is the loaded catalyst metal onto the working surface electrode (0.13 mg cm^{-2}). Q_H can be estimated by Eqs. (4) [7, 8]:

$$Q_H=\frac{1}{\nu A}\int I_{(V)}dV \quad \text{(Eq. (4))}$$

Where I (A) represents the peak current; V (V) is the peak potential; ν (mV s^{-1}) denotes the scanning rate, which is 25 mV s^{-1} in this experiment; and A (cm^{-2}) is the GCE's geometric area, which is 0.1964 cm^{-2}.

Turnover frequency (TOF) calculation

The pre-site TOF value was calculated according to the following Eqs. (5-8) [9-12]

$$TOF\left(H_2\,s^{-1}\right)=\frac{\#\text{total hydrogen turnovers per geometric area}}{\#\text{active sites per geometric area}} \quad \text{(Eq. (5))}$$

The number of total hydrogen turnovers was estimated from the current density extracted from

the LSV polarization curves according to:

$$\#\,\text{total hydrogen turnovers} = (|j|\frac{\text{mA}}{\text{cm}^2})\left(\frac{1\text{C s}^{-1}}{1000\,\text{mA}}\right)\left(\frac{1\,\text{mol e}^{-1}}{96485.3\,\text{C}}\right)\left(\frac{1\,\text{mol}}{2\,\text{mol e}^{-1}}\right)\left(\frac{6.022*10^{23}\,\text{molecules H}_2}{1\,\text{mol H}_2}\right) \quad \text{(Eq. (6))}$$

$$= 3.12*10^{15}\,\frac{\text{H}_2\,\text{s}^{-1}}{\text{cm}^2}\,\text{per}\,\frac{\text{mA}}{\text{cm}^2}$$

The number of active sites in Pt-based catalysts was calculated from the mass loading on the working electrode, the Pt contents, and the Pt atomic weight, assuming each Pt center accounts for one active site:

$$\#\,\text{active sites} = \left(\frac{\text{catalyst loading per geometric area } (x\,\text{g cm}^{-2})*\text{Pt wt\%}}{\text{Pt M}_\text{W}\,(\text{g mol}^{-1})}\right)\left(\frac{6.022*10^{23}\text{Pt atoms}}{1\,\text{mol Pt}}\right) \quad \text{(Eq. (7))}$$

$$= \left(\frac{0.13*10^{-3}\,\text{g cm}^{-2}\,\text{x}\,8.51\,\text{wt\%}}{195.084\,\text{g mol}^{-1}}\right)\left(\frac{6.022*10^{23}\,\text{Pt atoms}}{1\,\text{mol Pt}}\right) = 3.41*10^{16}\,\text{Pt sites per cm}^2$$

Finally, the current density from the LSV polarization curve can be converted into TOF values according to:

$$\text{TOF } (\text{H}_2\ \text{s}^{-1}) = \left(\frac{3.12*10^{15}}{3.41*10^{16}}*|\,j\,|\right) = 0.091*|j| \quad \text{(Eq. (8))}$$

Tafel Slope Calculation for MOR

The kinetic parameter of electrocatalyst for MOR was calculated by Tafel equation (9)[13, 14]

$$\eta = a + b\log i = -\frac{2.3RT}{\alpha nF}\log i_0 + \frac{2.3RT}{\alpha nF}\log i \quad \text{(Eq. (9))}$$

where R is gas constant, T (K) represents the absolute temperature, α is the charge transfer coefficient, F is the Faraday constant, i_0 (mA cm^{-2}) is the exchange current density.

Results and Discussion

Table S1. XRD determined structural parameters of AgPt NCs/C and Pt NPs/C (E-TEK).

Catalysts	$d_{(hkl)}$[(a)] Å			$D_{(hkl)}$[(b)] nm			$H_{(111)}/H_{(200)}$	$H_{(111)}/H_{(220)}$
	(111)	(200)	(220)	(111)	(200)	(220)		
AgPt NCs/C	2.31	2.02	1.40	3.19	2.13	2.49	2.96	7.50
Pt NPs/C (E-TEK)	2.27	1.98	1.39	2.16	1.89	2.11	2.91	6.02

[(a)] *Calculation from Bragg's law.*
[(b)] *Calculation from Debye-Scherrer's equation.*

Table S2. A comparison of HER activity of recently reported catalysts in acidic electrolytes.

Catalysts	Overpotential[(a)] @ 10 mA cm^{-2}	Tafel Slope[(a)] mV dec^{-1}	Ref.
AgPt NCs/C	16.61	19.05	This work
Pt NPs/C (E-TEK)	21.30	21.37	This work
S-doped AuPdPt NWs	12	17.7	[15]
Commercial Pt NPs/C	29	25.2	[15]
$Pt/PtTe_2/NiCoTe_2$/NPFC HFSs	36	23	[16]
$Pt_{68}Ag_{32}$ NDs	51	39	[17]
Pt/GNs	25	33	[18]
$Pt/PtTe_x$ NRs	44	23	[19]
$Pt/NBF\text{-}ReS_2/Mo_2CT_x$	29	24	[20]
AgPt HANS	69	40	[21]
Pt_1/Co_1NCs	4.15	17	[11]
Pt-PMo/ZIF-67-800	26	30	[22]
Pt_8Co	26.1	34	[23]
Pt_4Co_1 hollow sphere	14.8	27.45	[24]
$Pt/MoS_2/CF_s$	5	53.6	[25]
$Pt_{0.44}V$/3DHPNG/Au_{pla}/GCE	12	26.8	[26]
PtNPs/3DHPNG/Aupla/GCE	10	25.2	[26]
PtAg NFs/rGO	55	31	[27]
PtNi/Pt DNPs	21	23	[28]

[(a)] *Calculation from LSV curves in N_2-saturated 0.5 M H_2SO_4 aqueous solution.*

Table S3. A comparison of MOR performance of various Pt-based catalyst in acidic media.

Catalysts	ECSA[(a)] $m^2 g_{Metal}^{-1}$	Current density[(b)] mA cm^{-2}	I_f/I_b[(b)]	Ref.
AgPt NCs/C	81.36	22.65	1.47	This work
Pt NPs/C (E-TEK)	70.83	20.91	0.85	This work
$Pt_{9.8}Ru_1$/PANI/CNTs	-	26.01	1.36	[29]
$Pt_1Pb_2Ru_{0.5}$	43	9.83	1.52	[30]
Commercial Pt NPs/C	-	7.29	0.65	[30]
o-PtPd/rGO	-	22.76	1.56	[31]
Pt/AC-MWCNT	55.8	27.02	0.92	[32]
Pt/C-OT-4	78.66	17.48	1.82	[33]
PtRu/rGO-2	69.21	17.9	1.90	[34]
Pt_2Ir/MWCNT	85.30	9.72	1.10	[35]
PtO_x/CoO_y@OC-700	10.9	24.387	-	[36]

[(a)]Calculation from CV curves in N_2-saturated 0.5 M H_2SO_4 aqueous solution.
[(b)]Calculation from CV curves in N_2-saturated 0.5 M H_2SO_4 + 1 M CH_3OH aqueous solution.

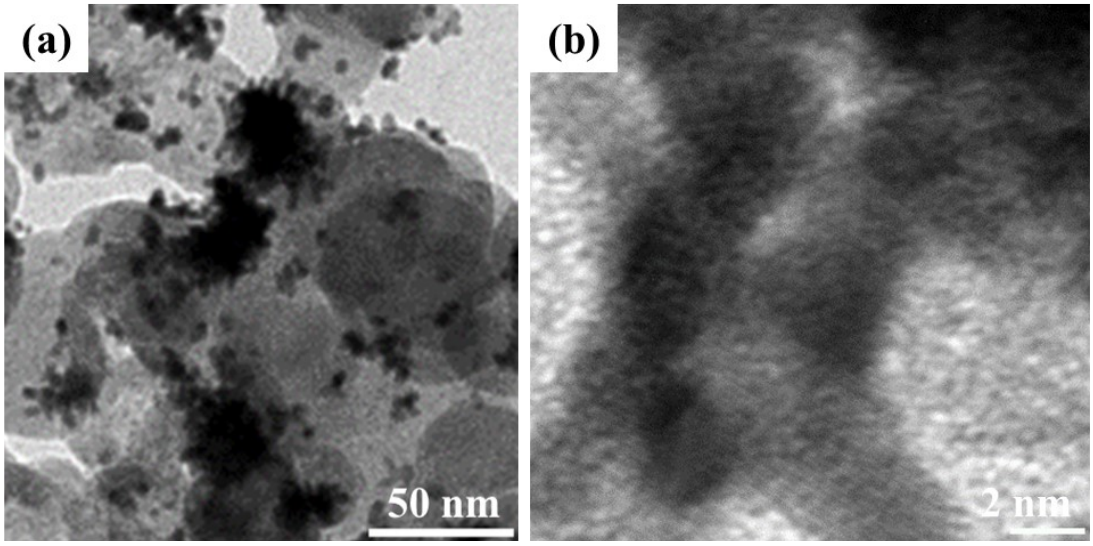

Figure S1. (a) TEM and (b) HR-TEM images of the AgPt NCs/C catalyst after CA test.

Table S4. The MOR performance of electrocatalyst before and after 2000-cycling tests.

Catalysts	Methanol electro-oxidation				
	Current density[(a)] mA cm^{-2}		I_f/I_b[(a)]		Deterioration %
	Initial	2000 cycles	Initial	2000 cycles	
AgPt NCs/C	22.65	18.68	1.47	1.45	17.52
Pt NPs/C (E-TEK)	20.91	14.90	0.85	0.79	28.74

[(a)]Calculation from CV curves in N_2-saturated 0.5 M H_2SO_4 + 1 M CH_3OH solution before and after 2000 cycling test.

References

1. Bhalothia, D.; Fan, Y.-J.; Lai, Y.-C.; Yang, Y.-T.; Yang, Y.-W.; Lee, C.-H.; Chen, T.-Y., *Nanomaterials* **2019,** *9* (7), 1003.
2. Huang, T.-H.; Bhalothia, D.; Dai, S.; Yan, C.; Wang, K.-W.; Chen, T.-Y., *Sustain. Energy Fuels* **2021,** *5* (11), 2960-2971.
3. Vargas-Ordaz, M.; Velázquez-Hernández, I.; Bañuelos, J. A.; Ledesma-García, J.; Álvarez-Contreras, L.; Arjona, N.; Guerra-Balcázar, M., *Mater. Today Energy* **2019,** *14*, 100335.
4. Zhang, C.; Zhang, Y.; Xiao, H.; Zhang, J.; Li, L.; Wang, L.; Bai, Q.; Liu, M.; Wang, Z.; Sui, N., *Colloids Surf. A Physicochem. Eng. Asp.* **2021,** *612*, 125960.
5. Huang, X.; Chen, Y.; Zhu, E.; Xu, Y.; Duan, X.; Huang, Y., *J. Mater. Chem. A* **2013,** *1* (46), 14449-14454.
6. Zhang, G.; Yang, Z.; Zhang, W.; Hu, H.; Wang, C.; Huang, C.; Wang, Y., *Nanoscale* **2016,** *8* (5), 3075-3084.
7. He, Y.; Chen, W.; Li, X.; Zhang, Z.; Fu, J.; Zhao, C.; Xie, E., *ACS Nano* **2013,** *7* (1), 174.
8. Li, N.; Tang, S.; Pan, Y.; Meng, X., *Mater. Res. Bull.* **2014,** *49*, 119-125.
9. Benck, J. D.; Chen, Z.; Kuritzky, L. Y.; Forman, A. J.; Jaramillo, T. F., *ACS Catal.* **2012,** *2* (9), 1916-1923.
10. Kibsgaard, J.; Jaramillo, T. F., Molybdenum Phosphosulfide: An Active, Acid-Stable, Earth-Abundant Catalyst for the Hydrogen Evolution Reaction. *Angew. Chem. Int. Ed.* **2014,** *53* (52), 14433-14437.
11. Chen, Y.; Ding, R.; Li, J.; Liu, J., *Appl. Catal. B: Environ.* **2022,** *301*, 120830.
12. Fei, H.; Dong, J.; Arellano-Jiménez, M. J.; Ye, G.; Dong Kim, N.; Samuel, E. L. G.; Peng, Z.; Zhu, Z.; Qin, F.; Bao, J.; Yacaman, M. J.; Ajayan, P. M.; Chen, D.; Tour, J. M., *Nat. Commun.* **2015,** *6* (1), 8668.
13. Huang, T.; Mao, S.; Zhou, G.; Zhang, Z.; Wen, Z.; Huang, X.; Ci, S.; Chen, J., *Nanoscale* **2015,** *7* (4), 1301-1307.
14. Lee, S.; Kim, H. J.; Choi, S. M.; Seo, M. H.; Kim, W. B., *Appl. Catal. A: Gen* **2012,** *429-430*, 39-47.
15. Zhang, X.; Wang, S.; Wu, C.; Li, H.; Cao, Y.; Li, S.; Xia, H., *J. Mater. Chem. A* **2020,** *8* (45), 23906-23918.
16. Yi, M.; Hu, S.; Lu, B.; Li, N.; Zhu, Z.; Huang, X.; Wang, M.; Zhang, J., *J. Alloys Compd.* **2021,** *884*, 161042.
17. Chen, S.-S.; Nan, L.-J.; Feng, J.-J.; Zhang, L.; Fang, K.-M.; Luo, X.; Wang, A.-J., *Int. J.*

Hydrog. Energy **2018,** *43* (12), 6096-6106.
18. Yan, X.; Li, H.; Sun, J.; Liu, P.; Zhang, H.; Xu, B.; Guo, J., *Carbon* **2018,** *137*, 405-410.
19. Chen, J.; Qin, M.; Ma, S.; Fan, R.; Zheng, X.; Mao, S.; Chen, C.; Wang, Y., *Appl. Catal. B: Environ.* **2021,** *299*, 120640.
20. Yi, M.; Li, N.; Lu, B.; Li, L.; Zhu, Z.; Zhang, J., *Energy Storage Mater.* **2021,** *42*, 418-429.
21. Shao, F.-Q.; Feng, J.-J.; Yang, Z.-Z.; Chen, S.-S.; Yuan, J.; Wang, A.-J., *Int. J. Hydrog. Energy* **2017,** *42* (39), 24767.
22. Wang, S.; Cao, Y.; Jia, W.; Lu, Z.; Jia, D., *Appl. Catal. B: Environ.* **2021,** *298*, 120579.
23. Hu, J.; Fang, C.; Jiang, X.; Zhang, D.; Cui, Z., *Inorg. Chem. Front.* **2020,** *7* (22), 4377.
24. Wei, M.; Huang, L.; Huang, S.; Chen, Z.; Lyu, D.; Zhang, X.; Wang, S.; Tian, Z. Q.; Shen, P. K., *J. Catal.* **2020,** *381*, 385-394.
25. Hou, D.; Zhou, W.; Liu, X.; Zhou, K.; Xie, J.; Li, G.; Chen, S., *Electrochim. Acta* **2015,** *166*, 26-31.
26. Zhang, Y.; Liu, L.; Sun, C.; Du, Y.; Zhou, Y.; Xie, Q., *J. Alloys Compd.* **2021,** *888*, 161564.
27. Liu, Q.; He, Y.-M.; Weng, X.; Wang, A.-J.; Yuan, P.-X.; Fang, K.-M.; Feng, J.-J., *J. Colloid Interface Sci.* **2018,** *513*, 455-463.
28. Li, L.; Wang, S.; Xiong, L.; Wang, B.; Yang, G.; Yang, S., *J. Mater. Chem. A* **2019,** *7* (20), 12800-12807.
29. Zhang, X.; Ma, J.; Yan, R.; Cheng, W.; Zheng, J.; Jin, B., *J. Alloys Compd.* **2021,** *867*, 159017.
30. Liao, W.; Zhou, S.; Wang, Z.; Liu, F.; Cao, J.; Wang, Q., *Fuel* **2022,** *308*, 122073.
31. Yang, C.; Zhang, D.; Zhao, W.; Cui, M.; Liang, R.; Ou, Q.; Zhang, S., *J. Alloys Compd.* **2020,** *835*, 155334.
32. Bhuvanendran, N.; Ravichandran, S.; Peng, K.; Xu, Q.; Khotseng, L.; Su, H., *Appl. Surf. Sci.* **2021,** *565*, 150511.
33. Chang, X.; Dong, F.; Yang, S.; Tang, Z.; Zha, F., *Int. J. Hydrog. Energy* **2019,** *44* (39), 21559-21568.
34. Shi, Y.; Zhu, W.; Shi, H.; Liao, F.; Fan, Z.; Shao, M., *J. Colloid Interface Sci.* **2019,** *557*, 729-736.
35. Bhuvanendran, N.; Ravichandran, S.; Zhang, W.; Ma, Q.; Xu, Q.; Khotseng, L.; Su, H., *Int. J. Hydrog. Energy* **2020,** *45* (11), 6447-6460.
36. Ding, C.; Dong, F.; Tang, Z., *J. Electroanal. Chem.* **2021,** *895*, 115487.